PNAS RESEARCH ARTICLE | PLANT BIOLOGY

LUMINIDEPENDENS orchestrates global transcriptional repression in *Arabidopsis*

Clara Bergis-Ser[a,1], Qingyi Wang[a], Xiaoning He[a], Maherun Nisa[a], Vickie Kaiser[a], Christelle Mazubert[a], Jeannine Drouin-Wahbi[a], Rim Brik-Chaouche[a], Layla Chmaiss[a], Jelle Van Leene[b,c], Geert De Jaeger[b,c], Jose Gutierrez-Marcos[d], Catherine Bergounioux[a], Clara Bourbousse[e,f], David Latrasse[a], Moussa Benhamed[a,g,h], and Cécile Raynaud[a,2]

Affiliations are included on p. 11.

Edited by Caroline Dean, John Innes Centre, Norwich, United Kingdom; received October 2, 2025; accepted November 4, 2025

Genomic integrity is constantly challenged by transcription/replication conflicts, a major source of replication stress and instability across all life forms. While extensive studies have elucidated mechanisms for resolving transcription/replication conflicts in animals, yeast, and prokaryotes, their counterparts in plants remain largely unexplored. Through a forward genetic screen, we identified LUMINIDEPENDENS (LD), previously known for its role in regulating the flowering repressor *FLC*, as a key factor in mitigating replication stress in plants. Notably, transcriptomic analyses reveal that LD loss results in the upregulation of over half of the *Arabidopsis* genes, placing LD as a global transcriptional repressor. Consistent with this role, LD directly binds a substantial portion of the *Arabidopsis* genome and interacts with the MED18 subunit of the Mediator complex to modulate RNA polymerase II phosphorylation. These findings uncover a fundamental function of LD in fine-tuning transcription at a genome-wide scale, with potentially an additional role in suppressing transcription–replication conflicts by locally dampening transcription and promoting replication fork progression. Our work highlights an intriguing genome-protective strategy in plants, that could shed light on mechanisms involved in transcription–replication conflict management in eukaryotic systems.

transcription | replication stress | RNA polymerase

Significance

In a genetic screen designed to identify regulators of the plant replication stress response, we identified the LUMINIDEPENDENS (LD) protein. By combining data obtained through genetic, transcriptomic and epigenomic approaches, we show that loss of LD or its partner FLD mitigate developmental defects caused by replication stress. Beyond this potential role during DNA replication, we show that these two proteins are general repressors of transcription, likely acting through their interaction with the Mediator complex and modulating RNA Pol II activity.

In all living organisms, nucleic acid transactions, including DNA replication and transcription, are major sources of DNA lesions due to replication errors, formation of DNA breaks, DNA–protein crosslinks, or torsional tensions induced by the replication or transcription process (1, 2). Consequently, replication stress (RS) caused by stalling of the replication machinery due to obstacles on the DNA template is an important cause of genomic instability in proliferating cells. In mammals, RS is a hallmark of cancer cells triggering the accumulation of mutations while also rendering tumor cells sensitive to drugs targeting the DNA damage response (DDR) pathway (3). Moreover, RS is also increasingly recognized as a key determinant in aging (4). In plants, the spontaneous occurrence of replication stress has not been investigated in detail. However, the DDR triggered by RS is highly conserved with that of animals as its response depends on the ATR kinase that activates the transcriptional regulator SOG1, a functional homolog of p53, which controls the expression of cell cycle regulators and DNA repair genes (5). In agreement with its role in RS response, ATR is essential to the viability of *Arabidopsis pol2a* mutants as they display constitutive RS due to the partial inactivation of the replicative DNA polymerase ε (6). By contrast, although SOG1 contributes to the RS response, it is not required for the viability of *pol2a* mutants, thus suggesting that other pathways function downstream of ATR and independently of SOG1 in plants (6). Indeed, E2F transcription factors act in concert with SOG1 to fine-tune the expression of RS-induced genes and to activate the WEE1 kinase (7). The latter contributes to the RS response by phosphorylating various targets controlling proteolysis or alternative splicing, thereby leading to cell cycle arrest (8–10). Interestingly, under control conditions, the RS response seems to be dispensable for vegetative growth in *Arabidopsis* since *atr* null mutants show no developmental defects (11). By contrast, loss of ATR severely affects embryo development and growth in maize and barley (12, 13), suggesting that RS is ubiquitous in plants, like in mammalian cells. Thus, former studies indicate that plant RS responses are mediated by an intricate set of regulatory layers and signaling pathways, of which more actors likely remain to be identified.

RS can be largely regarded as an inevitable consequence of normal cellular activities. Indeed, encounters between the replisome and the transcription machinery, termed transcription–replication conflicts (TRCs), are considered major sources of genomic

Author contributions: C.B.-S., G.D.J., C. Bergounioux, C. Bourbousse, D.L., M.B., and C.R. designed research; C.B.-S., M.N., V.K., C.M., J.D.-W., R.B.-C., L.C., J.V.L., C. Bergounioux, D.L., and C.R. performed research; J.G.-M. and C. Bourbousse contributed new reagents/analytic tools; C.B.-S., Q.W., X.H., M.N., J.V.L., G.D.J., C. Bergounioux, M.B., and C.R. analyzed data; and C.B.-S., G.D.J., J.G.-M., M.B., and C.R. wrote the paper.

The authors declare no competing interest.

This article is a PNAS Direct Submission.

[1]Present address: Université de Sherbrooke, Faculté de Médecine et des Sciences de la Santé, Département de Biochimie et de génomique fonctionnelle, Sherbrooke, Québec J1H 5N4, Canada.

[2]To whom correspondence may be addressed. Email: cecile.raynaud@universite-paris-saclay.fr.

This article contains supporting information online at https://www.pnas.org/lookup/suppl/doi:10.1073/pnas.2527372122/-/DCSupplemental.

Published December 2, 2025.

instability, particularly when they occur in the head-on (HO) orientation (14, 15). Various mechanisms have been described to limit or resolve TRCs in both prokaryotic and eukaryotic genomes. First, genome structure has been shaped through evolution to co-orient transcription with the direction of DNA replication, thereby limiting HO-TRCs (16, 17), especially in the case of highly transcribed genes. In addition, transcription and replication are largely anticorrelated during S-phase (18, 19). Yet, transcription and replication cannot be mutually exclusive since replication origins are enriched in the TSS of transcriptionally active genes (20). Thus, several mechanisms contribute to the resolution of TRCs, which act both on the replisome to allow replication restart and on RNA polymerases (RNAP) to reduce transcription locally through RNAP removal, resolution of R-loops (tripartite 3D structures composed of an RNA:DNA hybrid and a displaced single-stranded DNA), and modulation of chromatin organization (15, 21).

The mechanisms limiting TRCs in plants have been poorly investigated, but could involve the modulation of histone modifications (22). As in other eukaryotes, transcriptional activity is promoted by histone acetylation (23), whereas histone methylation either promotes or represses transcription depending on the modified lysine. In euchromatin, H3K4me3 correlates with active transcription, and defects in H3K4me3 deposition by the RNA Polymerase II–associated complex COMPASS result in defects in gene expression (24). By contrast, H3K4me1 and H3K4me2 are thought to promote or repress gene expression depending on the context (25). Whether impinging on these modifications could play a role in mitigating RS by avoiding or resolving TRCs is to date unknown. Nevertheless, several lines of evidence point to a dual role of the FLD/LD/SDG26 complex in the control of transcription and replication fork progression. This complex was originally identified for its role in the autonomous pathway controlling flowering time (26–28). FLD is a homolog of the human demethylase LSD1, involved in the repression of the floral repressor *FLC* via the demethylation of H3K4me1 (28), while LD is a putative, albeit atypical, TF of the homeobox family (HB) (26, 27, 29), and SDG26 is a putative histone methyl-transferase, although whether its catalytic activity is required for *FLC* regulation remains unclear (30). Together, these three proteins allow long-lasting *FLC* silencing by promoting H3K4me1 removal and subsequent H3K27me3 deposition (31, 32). In addition, the genome-wide function of LD and FLD was extended to the regulation of transcription at convergent genes: According to this model, FLD removes the H3K4me1 mark at convergent transcription sites, thereby slowing down transcription (33). In parallel with this work, R-loop formation at the *FLC* locus has been shown to interfere with the progression of the replication fork, suggesting that factors controlling R-loop formation and *FLC* expression could play a role in mitigating TRCs (34). Consistently, loss of the FCA or FY proteins involved in R-loop resolution, and acting upstream of LD and FLD at the *FLC* locus, affects replisome progression genome-wide (34). However, the role of LD and FLD in this process has not yet been examined.

Through a genetic screen aimed at identifying novel regulators of the replication stress response, we identified LD as a suppressor of the *pol2a* mutant, which exhibits impaired cell cycle progression and reduced growth due to constitutive replication stress. Chromatin binding analysis and transcriptomic profiling unexpectedly revealed that LD functions as a global repressor of gene expression in *Arabidopsis*. This regulatory function operates independently of replication stress, uncovering a previously unrecognized role of the FLD–LD complex in the broad control of transcriptional activity.

Results

LD Is Involved in the Replication Stress Response. To identify factors involved in the DDR, we performed an EMS genetic screen to isolate suppressors of the *pol2a* mutant, in which replication stress response is constitutively activated, leading to reduced growth and early flowering (6, 35). We mutagenized seeds of *pol2a* mutants expressing the DDR reporter *pCYCB1;1::CYCB1;1D-box-GUS* (36). This enabled us to then screen for suppressors using two criteria: i) suppression of the growth phenotype of *pol2a* plants and ii) reduction in the accumulation of CYCB1;1, thus limiting the identification of flowering time suppressors only. One of these suppressors, named *soa225,* shows partially restored growth compared to *pol2a* and rescues its early flowering phenotype (Fig. 1*A* and *SI Appendix*, Fig. S1*A*). Furthermore, expression of *CYCB1;1* is also reduced compared to *pol2a* in both root and shoot meristems (Fig. 1 *B* and *C*). We identified by whole genome sequencing five nonsynonymous mutations that were genetically linked to the *soa225* phenotype (*SI Appendix*, Table S1). Among those, only one introduced a premature stop codon in the *LUMINIDEPENDENS* (*LD*) gene (*SI Appendix*, Fig. S1*B*). To confirm that mutations in *LD* induce replication stress suppression, we obtained a T-DNA insertion mutant (*ld-4*) (Fig. 1*A* and *SI Appendix*, Fig. S1 *C* and *D*), which showed notable delays in flowering time (*SI Appendix*, Fig. S1*A*). We then generated *ld-4 pol2a* double mutants and found that, as in *soa225*, this other *LD* mutant allele partially restored the growth defects typical of *pol2a* (Fig. 1*A* and *SI Appendix*, Fig. S1 *A* and *E*). Furthermore, crosses between *soa225* and *ld-4 pol2a* mutants confirmed that *soa225* and *ld-4* mutations were allelic (*SI Appendix*, Fig. S1*E*). Finally, both the *ld* and the *ld pol2a* mutant could be rescued by a GFP-tagged LD under the control of the native LD promoter (*pLD::LD-GFP*, *SI Appendix*, Fig. S1*E*), further validating the identification of *ld* as the causal mutation in the *soa225* mutant. Because the *soa225* mutant contains other mutations, further analyses were carried out using the *ld-4* allele (hereafter referred to as *ld*).

LD was previously characterized for its role in controlling flowering time (26), and we found that the early flowering phenotype of the *pol2a* mutant (35) is fully rescued by *ld* (*SI Appendix*, Fig. S1 *A* and *E*). To further demonstrate the role of LD in replication stress responses, we tested the sensitivity of *ld* to hydroxyurea (HU). We found that *ld* roots grown on 1 mM HU were significantly longer than those of WT plants, while being similar when grown in control medium (Fig. 1*D*), confirming that *ld* has a reduced sensitivity to replication stress. Further phenotypic characterization confirmed that the rosette area was partially restored in the *ld pol2a* mutant (Fig. 1*E*). In addition, we tested the sensitivity of *gigantea* (*gi*), another late flowering mutant, also shown to produce very large rosettes due to its late flowering (37). As shown in *SI Appendix*, Fig. S2, only *ld* showed tolerance toward HU, whereas *gi* was as sensitive as the wild-type. Thus, although some of the effects of the *ld* mutation on the growth of the *pol2a* mutant likely result from a biomass effect associated with flowering time, the specific sensitivity of *ld* to HU, that is not observed in *gi,* confirms that LD is specifically involved in replication stress.

Considering that LD accumulates at high levels in the nuclei of meristematic cells (27) and that *ld* mutants grow better than WT plants under replication stress conditions, we hypothesized that LD could play a role in the control of the cell cycle. To test this hypothesis, we measured the size of root meristems in WT (Col-0), *pol2a*, *ld,* and *ld pol2a* seedlings. We found that *ld pol2a* double mutants display partially restored meristem size compared to *pol2a* (Fig. 1 *F* and *G*). We have previously shown that growth defects in *pol2a* mutants are associated with dramatically delayed cell cycle

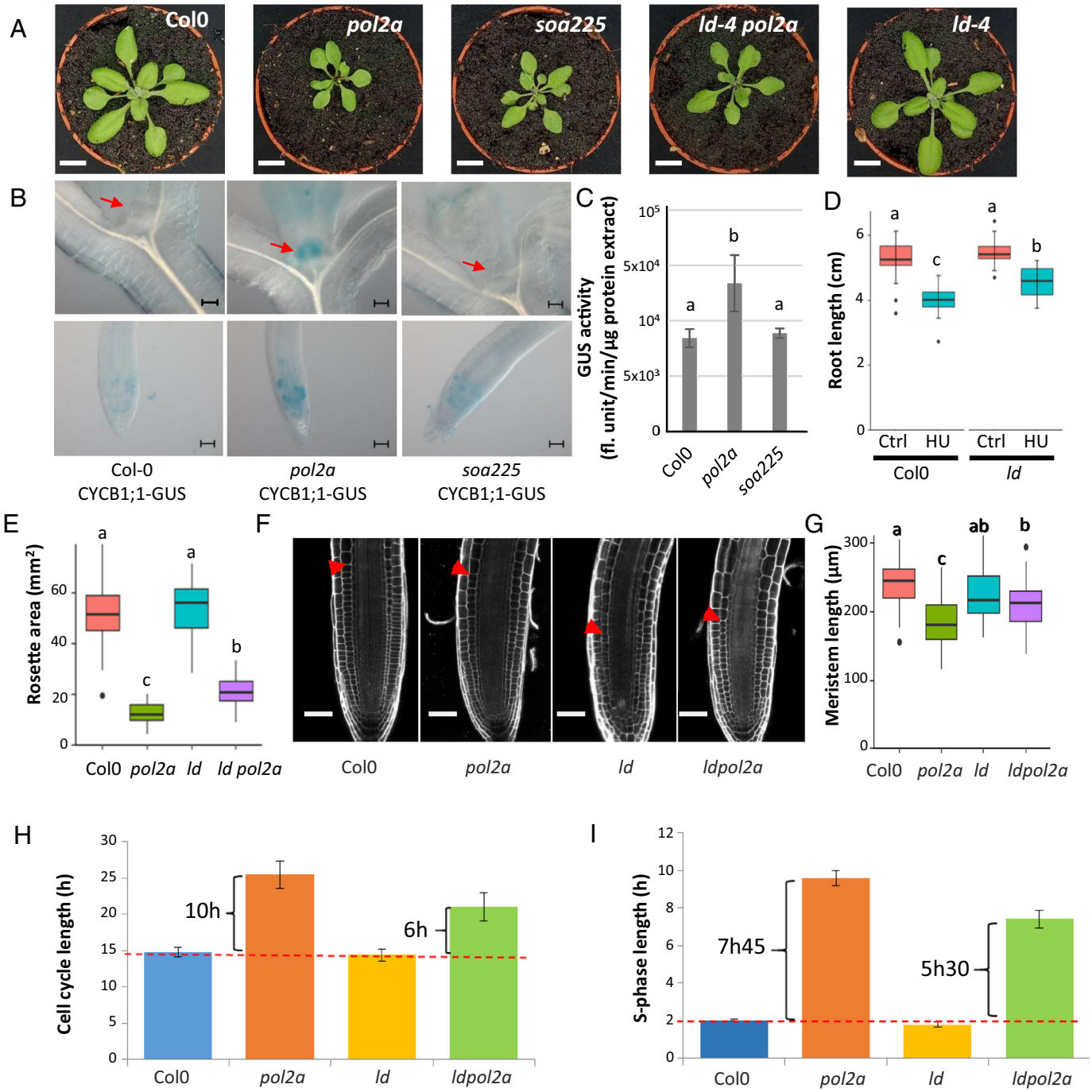

Fig. 1. LD is involved in replication stress response. (*A*) Phenotype of WT (Col0), *pol2a, ld, soa225,* and *ld pol2a plants. Pol2a* mutants display reduced size, *soa225* is the suppressor of *pol2a* isolated in the genetic screen, showing partial restoration of the *pol2a* growth defects. The *ld* mutant corresponds to the SAIL line SAIL_743_B07 which harbors a T-DNA insertion in the *ld* gene. Plants were grown in vitro for 10 d, and on soil for 14 d. (Scale bar, 1 cm for all panels.) (*B*) GUS-staining pattern obtained in the different mutant lines expressing the *CYCB1-1:GUS* construct. Red arrows indicate shoot meristems. GUS staining was increased in *pol2a* mutants and returned to lower levels in the *soa225* mutant. (Scale bar, 50 µm for all panels.) (*C*) Quantification of GUS activity (fluorescence unit/minute/µg of protein extract) in the indicated genotypes. Values are average +/- SD of three biological replicates; different letters indicate significantly different values (Wilcoxon sum-ranked test). (*D*) Root length measurement of 10-d-old Col0 and *ld* plantlets grown on ½ MS supplemented or not with hydroxyurea (HU, 1 mM). A Two-way ANOVA test was performed to compare genotypes, followed by a Tukey HSD test for multiple comparisons. Letters represent statistically different groups (P-value < 0.05, n > 20). This result is representative of 3 independent experiments. (*E*) Rosette area measurement of 24-d-old plants of the indicated genotypes. A Kruskal–Wallis test was performed to compare the genotypes, followed by a Wilcoxon rank-sum exact test for pairwise comparisons. Letters represent statistically different groups (P-value < 0.05, n ≥ 45). The partial restoration of *ld pol2a* phenotype seen in this graph is representative of 3 independent experiments. (*F*) Confocal images of 10-d-old meristems. Cell walls were stained with propidium iodide (10 µg/mL). Red arrows show the end of the meristematic zone. (Scale bar, 50 µm for all panels.) (*G*) Meristem length measurement of 10-d-old plantlets. A Two-way ANOVA test was performed to compare genotypes, followed by a Tukey HSD test for multiple comparisons. Letters represent statistically different groups (P-value < 0.05, n ≥ 34). This result is representative of 3 independent experiments. (*H*) Cell cycle length. (*I*) S-phase length in the indicated genotypes. The red dotted lines show cell cycle and S-phase length duration in the wild-type (Col-0). The error bars represent the SD between two independent experiments.

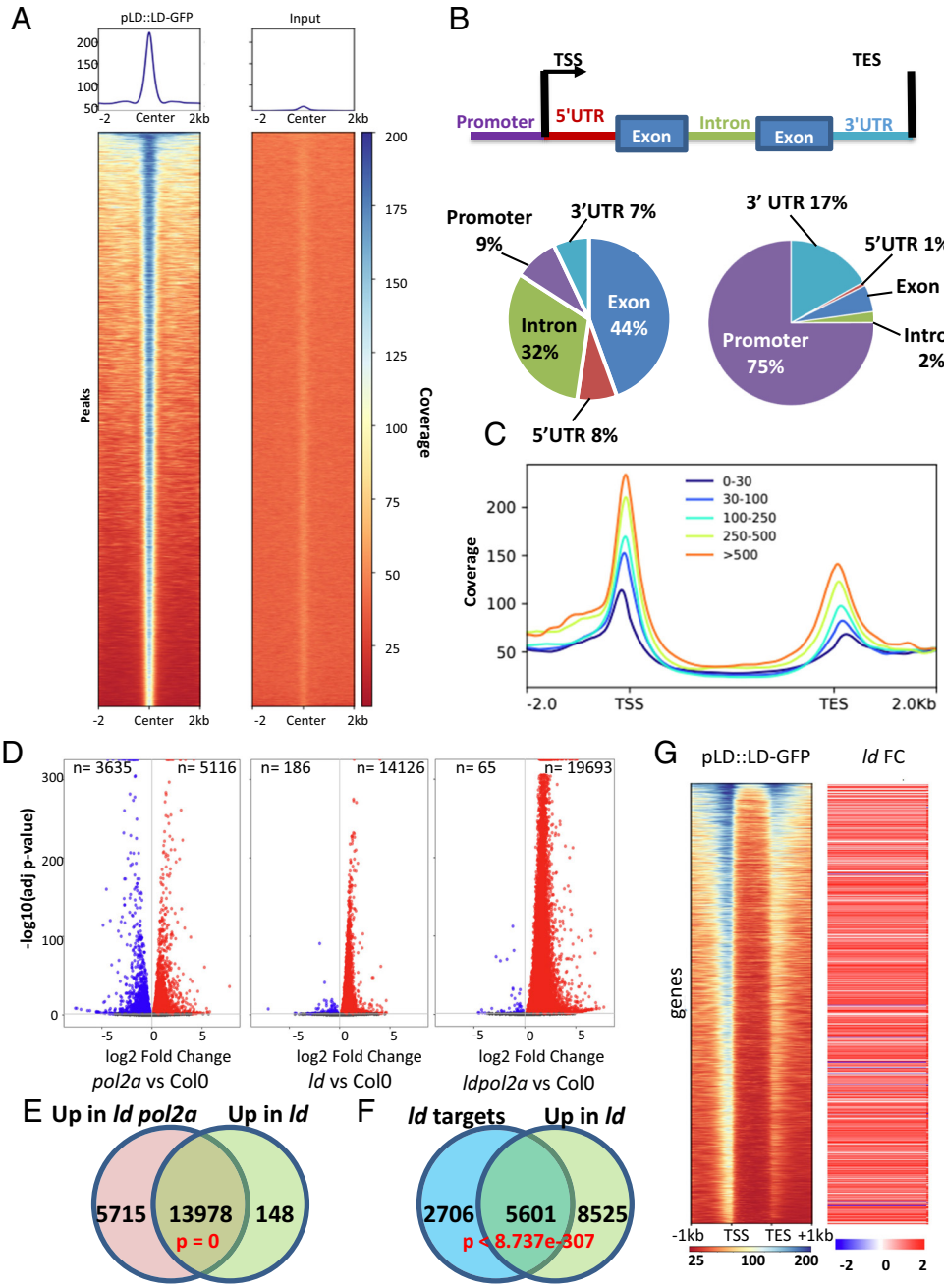

Fig. 2. LD is a global repressor of gene expression. (*A*) *Top*: Metaplot showing average LD binding profile centered on the peak's maximum obtained in the ChIP-seq analysis performed with *pLD::LD-GFP* lines. *Bottom*: Heatmap displaying ChIP signal at individual loci. The color gradient shows the sequence coverage in the ChIP data. The input is shown as a negative control. (*B*) Schematic representation of loci and pie charts comparing the proportion of promoter and genic sequences in the total *Arabidopsis* genome (TAIR 10 genome) (*Left*) and among LD binding sites (*Right*). (*C*) Metaplot showing the distribution of LD on its target genes. Genes were distributed between five quantiles of expression based on the number of read counts obtained in the wild-type. (*D*) Volcano plots summarizing the results of the spike-in RNAseq experiments. Significantly misregulated genes (adj *P*-value < 0.05) are shown as colored dots (blue = down-regulated genes, red = up-regulated genes). The *pol2a* mutant shows roughly the same number of up- and down-regulated genes compared to the wild-type. By contrast, *ld* and *ld pol2a* mutants show a global increase in gene expression. (*E*) Venn diagram showing the overlap between up-regulated genes in *ld* and *ld pol2a* mutants. The number of common up-regulated genes is higher than expected by chance (Fisher's exact test $P = 0$). (*F*) Venn diagram showing the overlap between LD targets identified by ChIP-seq and up-regulated genes in *ld*. The number of common up-regulated genes is higher than expected by chance (Fisher's exact test $P < 8.737e{-}307$). (*G*) Heatmap showing LD binding (*Left*) and the observed FC in *ld* on LD targets identified by ChIP-seq (*Right*).

progression (6). We therefore measured the cell cycle and S-phase length using cumulative EdU incorporation (38) to test whether cell cycle progression defects are rescued in *ld pol2a* mutants. As expected, we found the average cell cycle length to be 10 h longer and the average S-phase length to be increased by almost 8 h in *pol2a* mutants than in WT. Further, we found that the average length of the cell cycle was reduced by around 4 h (Fig. 1*H*) and that the average S-phase length was also shortened by about 2 h (Fig. 1*I*) in *ld pol2a* double mutants compared to *pol2a*. These results suggest that LD is involved in the induction of cell cycle checkpoints in response to replication stress. Taken together, these results support the view that the increased plant tolerance to replication stress in *ld* is mediated by the modulation of cell cycle progression.

LD Is a Bona Fide Repressor of Gene Expression. The LD protein harbors a putative Homeo-domain (27), suggesting it could function as a transcriptional regulator (29). We therefore attempted to identify its direct targets by chromatin immunoprecipitations. To this end, we complemented the *ld* mutant with the *pLD:LD-GFP* construct (*SI Appendix*, Fig. S1*E*) and found that LD-GFP protein was constitutively expressed, albeit at lower levels in mature organs (*SI Appendix*, Fig. S3). We generated data from two independent ChIP-seq experiments (*SI Appendix*, Fig. S4 *A* and *B*) and found over 8000 LD-targets (Fig. 2*A* and *SI Appendix*, Fig. S4*C* and Dataset S1). Most of LD-binding sites were found in gene promoters, accounting for 75% of its binding sites, despite promoter regions comprising only 9% of the *Arabidopsis* genome (Fig. 2*B*). Additionally, LD binds to both the 5′ and 3′ regions of its target genes (Fig. 2*C*). To analyze the relationship between LD binding and gene expression, we grouped genes in four quartiles based on their expression level, and plotted LD binding on each quartile (Fig. 2*C*), finding that LD binding correlates with gene expression. We then identified the sequence motives enriched at LD binding sites and found that instead of the typical homeobox

(HB) motif other sequence motives, such as bHLH/bZIP/BES1/E-box/BZR/Trihelix motives, GAGA repeats, WRKY, TCP, and HB-like, were associated with LD binding (*SI Appendix*, Fig. S4*D*). This diversity suggests that LD possesses a low sequence specificity and/or that it can be recruited to the chromatin independently of its putative DNA-binding domain. Next, we carried out a transcriptome analysis on shoot apices from WT (Col-0), *pol2a*, *ld,* and *ld pol2a* plants (Dataset S2) and found that despite the very large number of genes associated with LD binding, only 200 were differentially expressed in *ld* and not significantly enriched among LD targets (*SI Appendix*, Fig. S4*E*). Moreover, the majority of *pol2a* DEGs were also misregulated in the *ld pol2a* mutant, and the number of DEGs was actually higher in double mutant than in single mutant plants, indicating that LD loss of function does not restore wild-type gene expression levels in the *pol2a* mutant (*SI Appendix*, Fig. S5*A*). Furthermore, because *pol2a* mutants show constitutive activation of DDR genes (6, 7), we checked whether the *ld* mutation specifically restored the expression of these genes, but we did not observe significant restoration of DDR gene expression in *ld* plants (*SI Appendix*, Fig. S5*B*).

The very large number of putative LD targets, the lack of specificity among enriched TF binding motifs, the poor overlap between LD genomic binding sites and DEGs in the *ld* mutant and the absence of correlation between changes in gene expression and phenotypic rescue of the *ld pol2a* mutant compared to the *pol2a* mutant, prompted us to hypothesize that LD may affect gene expression globally rather than being involved in the regulation of specific genes. However, standard RNA-seq analysis is not suitable to detect a global change in mRNA accumulation (39, 40). To address this, we carried out an RNA-seq experiment including spike-in RNAs from Drosophila S2 cells, which allows mRNA data normalization (41). We found that *pol2a* plants had similar numbers of genes showing an increase and decrease in mRNA accumulation; however, both *ld* and *ld pol2a* displayed only an increase in transcript accumulation (Fig. 2*D* and Dataset S3 and *SI Appendix*, Fig. S6 *A–C*). In both *ld* and *ld pol2a* plants, the increase in transcript accumulation affected most genes in the genome (Fig. 2*D* and Dataset S3 and *SI Appendix*, Fig. S6 *A–C*), and the set of up-regulated genes was very similar between the two mutants (Fig. 2*E* and *SI Appendix*, Fig. S6*D*). This correlation was even more obvious when focusing only on LD targets identified by ChIP-seq (*SI Appendix*, Fig. S6*E*). Importantly, this increase in mRNA accumulation observed in *ld pol2a* cannot be attributed to higher levels of endoreduplication, since the increased endoreduplication observed in *pol2a* (6) was rescued by the *ld* mutation (*SI Appendix*, Fig. S6*F*). This global increase in mRNA levels also holds true for DDR-related genes (*SI Appendix*, Fig. S6 *G* and *H*), suggesting that the partial rescue of the *pol2a* phenotype results from this global reprogramming of DDR gene expression, rather than from a rescue of DDR activation. Taken together, our data suggest that LD plays a pivotal role in global mRNA production.

LD Directly Impinges on the Transcription Machinery. We next set to investigate the mechanism(s) by which LD modulates gene expression by carrying out an Affinity Purification assay coupled with Mass Spectrometry (AP-MS) based on the GS^{Rhino} tag (42, 43). These assays confirmed that LD interacts with FLD, SDG26, ELF2, ELF4, and APRF1 (30, 31, 44) (Table 1 and Dataset S4). Genetic analyses revealed that, similarly to *ld*, *fld* mutants could also suppress the growth defects and meristem length reduction commonly observed in *pol2a* plants (Fig. 3 *A–C*). Moreover, *fld* mutants exhibited increased mRNA accumulation

Table 1. LD Protein partners identified through AP-MS

Protein accession	Protein name	# Identified with min 2 peptides (in 3 replicates)	Affinity Enrichment Score
AT4G02560	LD|Homeodomain-like superfamily protein	3	156,585
AT1G72630	ELF4-L2|ELF4-like 2	3	116,724
AT1G17455	ELF4-L4|ELF4-like 4	3	107,562
AT3G10390	FLD, RSI1|protein FLOWERING locus D-like protein	3	71,351
AT5G14530	APRF1|Transducin/WD40 repeat-like superfamily protein	3	53,587
AT1G76710	ASHH1, SDG26|SET domain group 26	3	62,452
AT2G22370	MED18|Mediator of RNA polymerase II transcription subunit	2	976
AT1G07950	MED22B|Surfeit locus protein 5 subunit 22 of Mediator complex	3	313

Only previously known partners and interactors selected for further analysis are listed in this table. The full list of partners can be found in Dataset S4 *A* and *B*.
Affinity Enrichment Score is the product of the NSAF ratio vs the large dataset and the –log(*P*-value) of the *t* test.

to the same extent as *ld* plants (Fig. 3*D* and *SI Appendix*, Fig. S7). Furthermore, both mutations led to the up-regulation of highly similar gene sets (Fig. 3*E* and *SI Appendix*, Fig. S7 and Dataset S5). It is worth noting that between independent replicates of the spike-in RNAseq, the fold change observed for up-regulated genes displayed some variations. Nevertheless, the set of up-regulated genes was highly reproducible between experiments, and this was further confirmed by performing a third independent replicate of spike-in RNA seq on the *ld* mutant (*SI Appendix*, Fig. S8 and Dataset S6). Since loss of *ld* and *fld* have very similar consequences on mRNA accumulation, we took advantage of the publicly available ChIP-seq data for the FLD protein (33). As shown in Fig. 3*F*, genes targeted by LD also displayed FLD binding, and were up-regulated genes in *ld* and *fld*. Interestingly, LD was found to be enriched in the 5' region of the gene and to a lesser extent in the 3' region, whereas FLD showed clear enrichment in the 3' region (Fig. 3*F* and *SI Appendix*, Fig. S9 and Dataset S7), suggesting the presence of gene loops at these loci. Together, these findings suggest that LD and FLD act in concert to suppress transcriptional activity.

FLD is thought to modulate transcription speed at convergent genes by facilitating the removal of the H3K4me1 histone mark (33), but this process affects around 2,000 genes, which alone cannot account for the global increase in mRNA accumulation observed in *ld* and *fld*. We therefore investigated whether total H3K4me1 levels could be modified in *ld* mutants. Western blot analysis revealed that global H3K4me1 accumulation remained unchanged in *ld* (*SI Appendix*, Fig. S10*A*). Furthermore, the activating mark H3K9ac, which strongly correlates with gene activation, was present at similar levels in *ld* and wild-type plants (*SI Appendix*, Fig. S10*B*). Together, these findings suggest that LD could also modulate transcription through mechanisms that are independent of histone modifications. Indeed, in our AP-MS analysis, we identified several chromatin-associated proteins among LD partners, including chromatin readers, and a topoisomerase, consistent

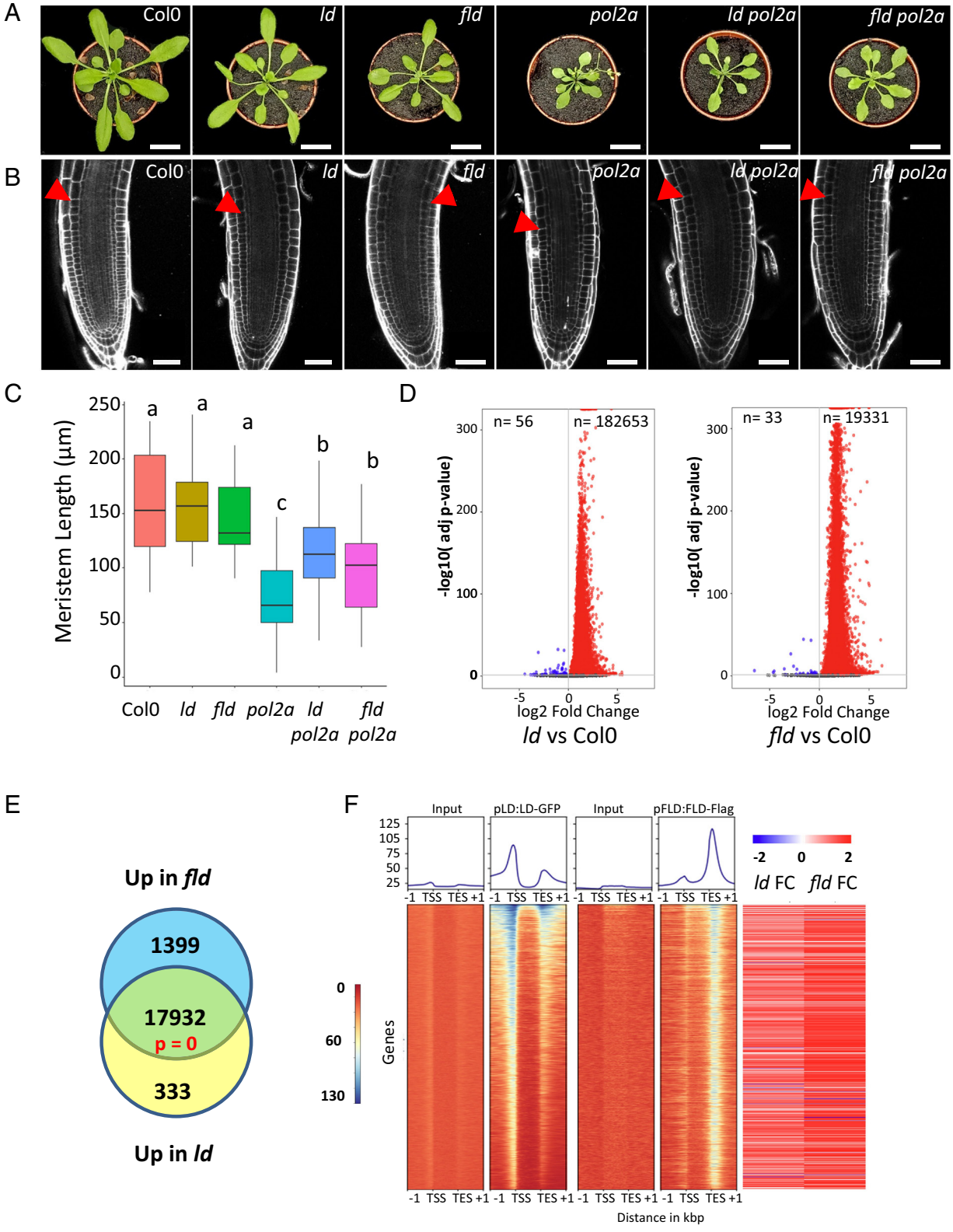

Fig. 3. LD and FLD likely function together during replication stress response. (*A*) Pictures showing the rosette size of the different mutants. Plants were grown in vitro for 10 d and then on soil for three weeks. *fld pol2a* has a partially restored rosette size compared to *pol2a*, like *ld pol2a*. (Scale bar, 2 cm for all panels.) (*B*) Confocal images of 10-d-old meristems. Plantlets were stained with propidium iodide (10 µg/mL), Red arrows show the end of the meristem zone. (Scale bar, 50 µm for all panels.) (*C*) Meristem length measurement of 10-d-old plantlets. A Kruskal–Wallis test was performed to compare the genotypes, followed by a Wilcoxon rank-sum exact test for pairwise comparisons. Letters represent statistically different groups (*P*-value < 0.05, n > 20). This result is representative of 2 independent experiments. (*D*) Volcano plots summarizing the results of the spike-in RNA-seq experiments. Significantly misregulated genes (adj *P*-value < 0.05) are shown as colored dots. (*E*) Venn diagram showing the overlap between up-regulated genes in *ld* and *ld pol2a* mutants. The number of common up-regulated genes is higher than expected by chance (Fisher's exact test $P = 0$). (*F*) Comparison of LD and FLD binding on genes identified as LD targets. *Left*: Metaplots (*Top*) and heatmaps (*Bottom*) showing LD or FLD binding profile centered on the genes obtained in the ChIP-seq data generated with *pLD:LD-GFP* lines and with *pFLD:FLD-flag* lines (33). The color gradient shows the sequence coverage in the ChIP data. The input is shown as a negative control for both experiments. *Right*: Heatmap showing the observed FC in *ld* and *fld* on the same genes.

with the finding that the effect of LD and FLD on the expression of convergent genes depends on Topoisomerase I (33). In addition, we found several proteins directly involved in transcription (Dataset S4), including MED18 and MED22, two subunits of the Mediator complex known for its role in promoting transcription initiation (45, 46). Bimolecular Fluorescence Complementation (BiFC) and yeast two-hybrid assays further confirmed that LD interacts with MED18 (Fig. 4*A* and *SI Appendix*, Fig. S11).

Since the Mediator complex is known to promote transcription initiation by facilitating RNA Pol II phosphorylation (45), we performed ChIP-seq experiments to determine whether RNA Pol II loading on chromatin is increased in *ld* mutants. Upon recruitment on gene promoters, RNA Pol II is initially phosphorylated on Ser5 of its C-Terminal repeat Domain (CTD) enabling transcription initiation. During elongation, Ser2 phosphorylation becomes predominant, and transcription termination is ultimately carried out by Ser2P RNA Pol II, after removal of Ser5P (47). To investigate RNA Pol II distribution in wild-type and *ld,* we performed ChIP-seq using specific antibodies for Ser2P and Ser5P RNA Pol II. To refine our analysis of Pol II occupancy, genes were categorized into five quantiles based on their expression levels in the *ld* mutant, as quantified by RNA-seq (*SI Appendix*, Table S2). We observed an increase of Ser5P RNA Pol II occupancy across all genes up-regulated in *ld*, with this effect becoming more pronounced in genes exhibiting higher expression levels (Fig. 4*B* and *SI Appendix*, Fig. S12). As expected, the levels of Ser2P RNA Pol II correlated with transcription, and a clear increase in Ser2P RNA Pol II occupancy was observed along the gene body of most highly expressed genes. These findings suggest that LD modulates transcription through its interaction with the Mediator complex and its influence on RNA Pol II phosphorylation.

Discussion

Transcriptional activity is intricately linked to genome integrity through multiple mechanisms. First, Transcription-Coupled DNA repair (TCR) serves as a key pathway for repairing small DNA lesions within transcribed regions (48). Second, RNA Damage sensing by the transcriptional machinery has recently emerged as a key element of the cellular response to genotoxic stress (49). Finally, the coordination of transcription and DNA replication is essential for minimizing transcription–replication conflicts, thereby ensuring efficient S-phase progression during the cell cycle (15). In this study, we identified a previously unrecognized function of LD in the replication stress response through a genetic screen. Specifically, *ld* mutants were isolated in a suppressor screen of the replicative stress mutants *pol2a,* and we further confirmed that LD loss enhances plant tolerance to replication stress (RS) using hydroxyurea treatment. Importantly, this effect was not observed in the *gi* mutant that also affects flowering time, confirming that the effect of LD on RS response is not linked to increased biomass production resulting from late flowering.

Genome-wide analysis of LD binding sites and gene expression changes in *ld* mutants revealed that LD functions not only in the RS response but also as a global negative regulator of transcription. More than 13,000 protein-coding genes were upregulated in the *ld* mutant, and LD was found to bind more than half of them. Since these analyses were conducted on whole *Arabidopsis* plantlets rather than exclusively on proliferating or S-phase cells, these findings suggest that LD limits transcription globally, independently of RS occurrence. In addition, genetic analyses confirmed that this transcriptional repressive function is shared by FLD, an LD interactor, suggesting that the LD-FLD complex, along with its previously characterized partners (30, 31), plays a key role in transcriptional repression. The mechanisms by which the LD-associated complex limits transcriptional activity may be diverse. This complex has been shown to reduce H3K4me1 and H3K36me3 levels at the *FLC* locus (31), and FLD-mediated H3K4me1 removal has been proposed to slow transcription at convergent genes (33). However, we did not detect a global increase in H3K4me1 levels that would correspond to the increased mRNA accumulation observed in *ld* mutants. This suggests that LD-dependent transcriptional control involves additional mechanisms beyond histone modifications.

Transcription operates as a cyclical process comprising initiation, elongation, termination, and the recycling of RNA polymerase II (RNA Pol II) to restart the cycle, with each step tightly regulated (50). Through AP-MS analysis, we identified LD as a copurifying partner of MED18 and MED22, two subunits of the Mediator complex. Furthermore, BiFC and yeast two-hybrid assays confirmed the LD–MED18 interaction. In *Arabidopsis*, the Mediator complex consists of at least 28 subunits (51) organized into three distinct modules: the head module, which interacts directly with RNA Pol II; the tail module, which engages with specific transcription factors; and the middle module, which bridges the two extremities and transmits regulatory signals from the tail to the core transcription machinery (45). MED18 and MED22 belong to the head module (45), and Mediator is essential for efficient transcription initiation and elongation (52), suggesting that LD may function in close proximity to RNA Pol II and modulate its activity. Consistently, ChIP-seq data reveal that LD binds mostly the promoter region of its target, and to a lesser extent their 3' end, while FLD is mostly found in the 3' region of their common targets. This suggests that LD and FLD play a role throughout the transcription cycle, possibly by impinging on RNA Pol II recycling that is favored by gene looping (53), reinforcing their potential function in transcriptional regulation beyond elongation.

Alongside its interaction with the Mediator complex, phosphorylation of the C-terminal repeat domain (CTD) of RNA Pol II serves as a key regulatory mechanism. RNA Pol II is initially recruited to promoters in its unphosphorylated form and phosphorylation at Ser5P enables transcription initiation, while Ser2 phosphorylation promotes elongation. Finally, Ser5P dephosphorylation facilitates transcription slowdown and termination (47, 50). Here, we found that RNA Pol II Ser5P levels were increased in *ld* mutants, suggesting that LD contributes to Ser5 dephosphorylation. Supporting this hypothesis, LD was recently proposed as a functional homolog of Ref2/PNUTS, a component of the Cleavage and Polyadenylation Specificity Factor (CPSF) (44). In yeast and metazoans, Ref2/PNUTS interacts with the protein phosphatase PP1 to regulate RNA Pol II Ser5 phosphorylation, thereby modulating the elongation rate (54). Until recently, no PNUTS homolog had been identified in *Arabidopsis*. However, LD was found to share structural features with PNUTS, and Ser5P levels were dramatically increased at the *FLC* locus in *ld* mutants (44).

Whether this LD-mediated regulation of Ser5P extended beyond *FLC* remained unclear. Here, we show that the increase in Ser5P levels is widespread across most upregulated genes in *ld* mutants, suggesting that LD regulates transcription at least in part through RNA Pol II phosphorylation. RNA Pol II activity is governed by a network of highly interconnected factors during transcription elongation. Proteins containing a TFIIS N-terminal domain interact with TND-interacting motif (TIM)-containing proteins, forming a dynamic network that links the transcription machinery, including the Mediator complex and the PNUTS/PP1

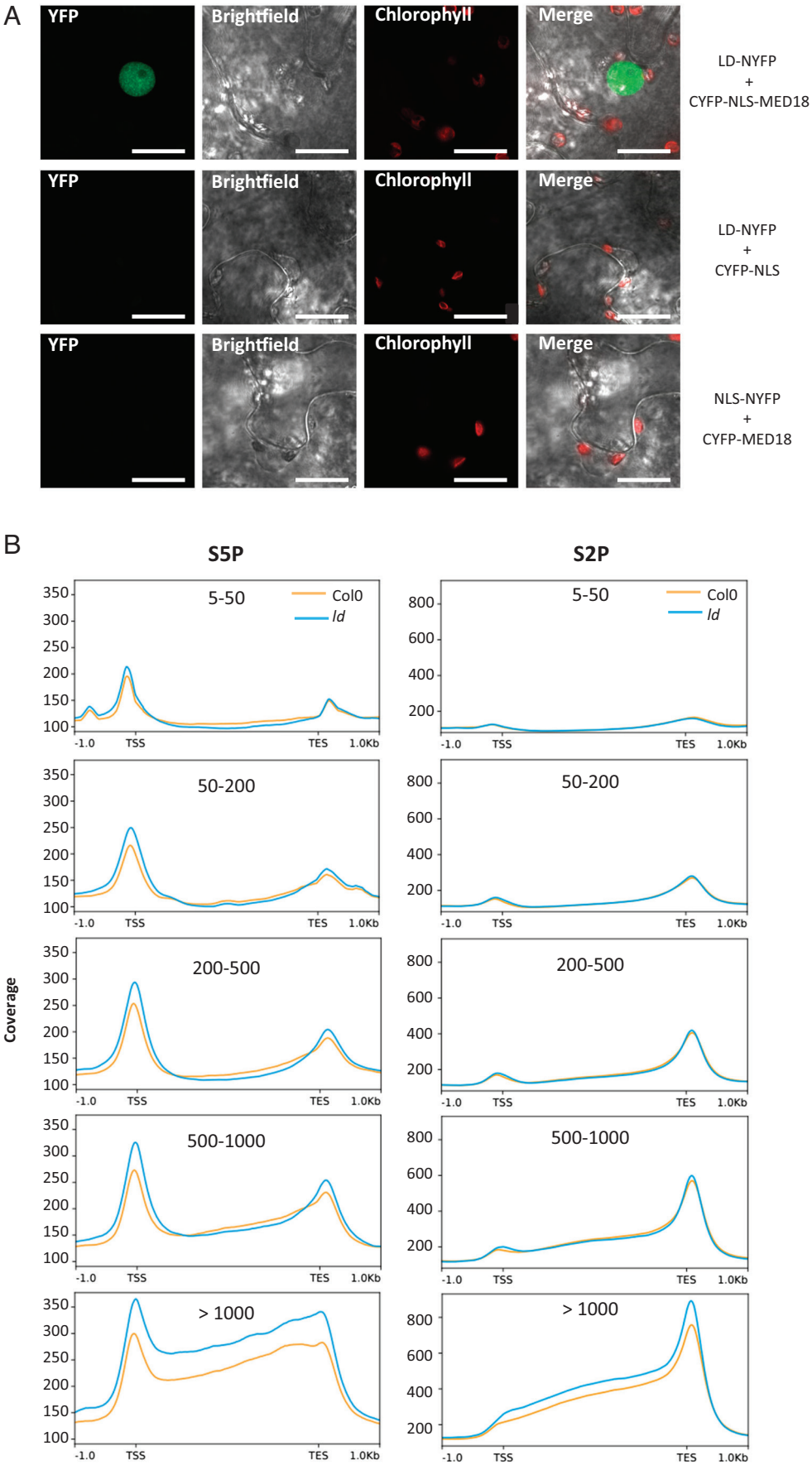

Fig. 4. LD modulates RNA Pol II activity through its ability to bind the MED18 subunit of the Mediator complex. (*A*) Confocal microscopy images showing BiFC experiments between LD and MED18; GUS was used as a negative control. (*B*) Metaplots showing RNA Pol II S5P and RNA Pol II S2P distribution over genes up-regulated in *ld*. Genes were distributed in 5 quantiles based on their expression in *ld*.

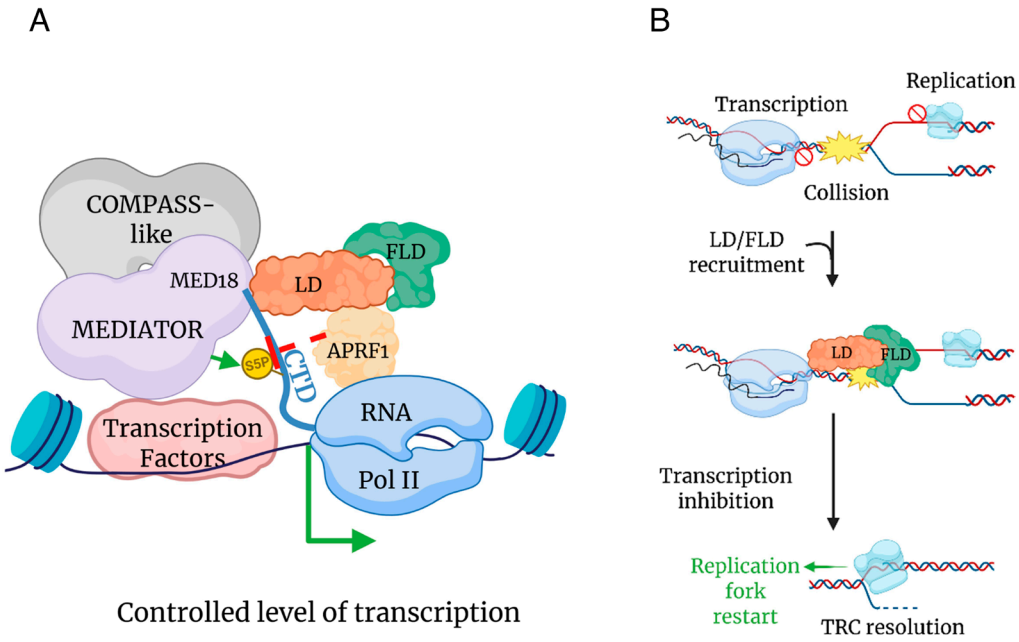

Fig. 5. Model describing the role of LD in the regulation of transcription. (*A*) A complex comprising LD and FLD, and most likely the APRF1 phosphatase, is recruited at transcription sites through the ability of LD to interact with the MED18 subunit of the Mediator complex. Dephosphorylation of S5P of RNA Pol II decreases transcription rate leading to controlled transcription levels (Created in BioRender. M. Benhamed (2025) https://BioRender.com/djlo9dk). (*B*) Working model for the role of LD and FLD during replication stress: After detection of collisions between the replication and transcription machinery, LD and FLD recruitment may allow transcription inhibition, TRC resolution, and replication restart (Created in BioRender. M. Benhamed (2025) https://BioRender.com/4rnq543).

complex (55). Notably, LD harbors a TFIIS domain, further supporting its potential role as PNUTS functional homolog. Under this model, LD recruitment to transcription sites via LD–MED18 interaction would facilitate Ser5P dephosphorylation, likely through APRF1 activity, thereby modulating transcription levels (Fig. 5*A*). However, two recent studies reported that PNUTS is essential for transcription, as its acute depletion via targeted protein degradation resulted in a global transcriptional decrease (56, 57). This contrasts sharply with the transcriptional upregulation observed in *ld* loss-of-function mutants in *Arabidopsis*, highlighting a major functional distinction between LD and PNUTS.

Along with MED proteins and APRF1, our IP-MS analysis revealed that LD could interact with several chromatin modifiers such as SUVR2, an ATRX-like protein of unknown function, DEK4, and the GTE4 protein. SUVR2 is involved in the RdDM pathway of gene silencing, and its activity is thought to go through its interaction with chromatin remodeling complexes, as its catalytic residues are dispensable for its activity (58). By contrast, GTE4 and DEK4 function as transcriptional activators (59, 60). Thus, the role of LD in transcriptional regulation likely involves highly complex interactions with both positive and negative regulators of gene expression. It is worth noting that caution for false positives and false negatives is always needed when interpreting interactomics results. Nevertheless, the large number of chromatin-associated proteins potentially associated with LD suggests that, in addition to its interaction with the Mediator complex and its impact on RNA Pol II phosphorylation, LD could also function through the modulation of histone modifications or chromatin remodeling, as suggested by (33).

Beyond its role as a global transcriptional repressor, our genetic analysis indicates that LD also plays a role in the replication stress (RS) response. It may be recruited to transcription–replication conflict (TRC) sites to attenuate transcription and facilitate TRC resolution (Fig. 5*B*), although this hypothesis will require further investigation. Interestingly, a DNA topoisomerase was identified among LD partners, further supporting our hypothesis that it could play a role in TRC resolution. The *ld* mutation was identified as a suppressor of the *pol2a* mutant, in which the RS response is constitutively activated, and *ld* mutants exhibit increased tolerance to hydroxyurea (HU). These findings appear paradoxical given LD's function as a transcriptional repressor, as the resolution or avoidance of transcription–replication conflicts (TRCs) generally requires transcriptional downregulation, and mutants deficient for these mechanisms are generally hypersensitive to replication stress. Indeed, in mammals, TRCs in rapidly proliferating cells are prevented by transcriptional repression through FOXD3 recruitment to highly expressed genes (61). More broadly, several mechanisms that facilitate RNA Pol II removal from the replication machinery are essential for limiting TRCs (62, 63), including PNUTS-mediated RNA Pol II degradation (64). However, unlike PNUTS-deficient cells, which exhibit replication defects even in the absence of exogenous RS (64), *ld* mutants do not display such defects, suggesting key functional differences between LD and PNUTS.

Two nonmutually exclusive mechanisms could explain the suppression of RS-induced defects in *ld pol2a* mutants. First, the global upregulation of gene expression, including that of cell cycle regulators, may shift the balance between cell cycle repressors and activators, thereby partially inactivating RS-triggered checkpoints. Second, we propose that RS leads to the downregulation of specific genes in S-phase cells via LD activation, and that LD loss prevents this repression, ultimately promoting improved plant growth. While future studies will be required to further elucidate LD's role in RS, we propose that LD primarily functions as a global transcriptional repressor, whose activity can be locally recruited under RS conditions to reinforce transcriptional silencing at TRC sites.

Materials and Methods

Plant Material and Growth Conditions. We used Columbia-0 (Col0) lines for WT plants, SAIL_743_B07 (*ld-4*) from the SAIL collection, and SALK_015053 (*fld*) from the SALK collection. The *gi-2* mutant has been described previously (37).

All mutants are in Col-0 background. Seeds were surface-sterilized in diluted Bayrochlore™ for about 25 min under agitation, then washed two times with sterile water and left in sterile water at 4 °C in the dark for 2 d. Seeds were then sown on ½ MS medium, with 1,1 g of Murashige and Skoog (MS) medium (Basalt salt Mixture M0221, Duchefa) and 4 g of Agar (Agar HP696, Kalys) in 500 ml of sterile water. Plants were grown for 10 din vitro and transferred to soil. For rosette area measurement, plants were placed one week in short day conditions (8 h light, 20 °C) and then transferred to long day conditions (16 h light, 21 °C). For other experiments, plants were directly placed under long day conditions in the greenhouse.

Molecular Cloning and Plant Transformation. Constructs encompassing the *LD* cDNA expressed under the control of the *LD* promoter were obtained using the GreenGate technology (65). The chosen LD promoter sequence corresponds to 1 kb upstream of the ATG. Similarly, GreenGate cloning was used to generate the LD-GS^{rhino} fusion for AP-MS, combining the RPS5a:XVE inducible promoter with the *LD* cDNA and the GS^{rhino} tag (66). Clones encompassing the 5′ and 3′ moieties of LD were purchased from Eurofins Genomics. After GreenGate assembly, constructs were introduced in Agrobacterium (ASE strain containing the pSOUP plasmid), and plants were transformed via the floral dip method (67). Primers used for cloning are listed in *SI Appendix*, Table S3. For BiFC experiments, the *LD* and *MED18* cDNAs were cloned in the pENTR3C and the pDONR221 vectors, respectively (Thermofisher Scientific™). Because the MED18 protein does not include a nuclear localization signal (NLS), a short fragment encoding an NLS was introduced upstream of MED18 in the pDON221 vector. LD and MED18 were then introduced in the pBIFP1 and pBIFP3 vectors, respectively. The same NLS sequence was cloned in the pENTR3C vector, and nuclear-targeted YFP moieties were used as negative controls.

EMS Mutagenesis. About 5,000 seeds were surfaced-sterilized with Bayrochlore™ and washed three times with sterile water. They were imbibed overnight at 4 °C in a 0.1% KCl solution (w/v). The next morning, EMS was added to the solution (final concentration 0.3% w/v), and seeds were incubated for only 7.5 h due to the high sensitivity of the *pol2a* mutant to genotoxins. Seeds were next washed twice with sodium thiosulfate (100 mM) for 15 min, and twice with sterile water for 15 min. Seeds were finally sown on MS medium and grown at 20 °C for two weeks. 2,000 plants were transferred to the greenhouse, and seeds were harvested by pools of 10 plants for subsequent phenotypic screening.

Root Growth Experiments. Four-day-old plantlets were transferred to new plates of ½ MS medium and ½ MS medium supplemented with 1 mM HU and aligned at the top of a square petri dish. They were then placed vertically in a growth chamber under long day conditions. After about one week, Petri dishes were scanned, and root length was measured using the Fiji software (https://imagej.net/software/fiji/). At least 20 roots were measured in each experiment. Three independent biological replicates were measured. Statistical analysis was conducted on the R 4.2.1 version software.

Rosette Area Measurement. Pots of different genotypes were randomized on trays in the growth chamber to avoid light or temperature bias. Rosette's pictures were taken for each genotype and analyzed in Fiji. Rosettes were filled with a homogeneous red color, and areas were selected with the wand tool. At least 40 rosettes were measured in each experiment. Three independent biological replicates were measured. Statistical analyses were conducted on the R 4.2.1 version software.

GUS Staining. Root and shoot meristems were placed in 100% cold acetone for 15 min, and GUS activity was as described in ref. 68. Plantlets were incubated at 37 °C for 1 h and then washed with 70% ethanol. Then, they were fixed with 4% PFA for 20 min under vacuum and cleared with a chloral hydrate solution at RT overnight. [8 g CCl3CH(OH)2 (Sigma), 2 ml of 50% glycerol anhydrous, and 1 ml of sterile water]. Images were taken with a NIKON, AZ100, and a video camera, Nikon RI1.

Confocal Microscopy. We used 10-d-old meristems stained for about 5 min in a propidium iodide (10 mM) bath. We used a laser with an excitation wavelength of 561 nm on a Zeiss LSM 880 laser scanning confocal microscope and imaged them by acquiring the fluorescence of emission wavelength between 560 and 700 nm, using an X20 lens. At least 20 meristems were measured per experiment. Three independent biological replicates were performed. For BiFC experiments, we used a laser with an excitation wavelength of 514 nm. YFP fluorescence was acquired between 520 and 570 nm, and chlorophyll autofluorescence was acquired between 620 and 720 nm.

EdU Labeling. Two lines of about 40 seeds were sown on square petri dishes containing ½ MS medium, and germinated vertically for 5 d. Liquid ½ MS medium supplemented with 10 μM EdU was poured on top of the roots until each root tip was covered with the solution. Plantlets were fixed at a minimum of four different time points, separated by a minimum of 2 h each, in 4% (w/v) PFA in 1X PME (0.5 M PIPES pH 6.9, 50 mM MgSO4, 10 mM EGTA) for 15 min inside Eppendorf tubes pierced on the cap, under a vacuum. Sample preparation and image acquisition were performed as described in (7). EdU-marked nuclei were counted in Fiji. At least 15 images with an average of 300 nuclei were used. Four independent biological replicates were measured. Statistical analyses were conducted on the R 4.2.1 version software.

Western Blotting. Nuclear proteins were extracted and separated on a Bolt 4 to 12% Bis-Tris Plus Wedgewell Gel under NuPage MES buffer conditions, with migration at 100 V for 1 h. Semidry transfer was performed using the iBlot® 2 Dry Blotting System. Molecular weight markers were established using the SeeBlue™ Plus2 prestained protein ladder, with sizes indicated on the left in kDa. Primary antibodies used were anti-H3 (ab1791, Rabbit, 1:20,000) and anti-H3K9ac (Millipore 07-352, Rabbit, 1:10,000), followed by a secondary anti-Rabbit IgG antibody conjugated with alkaline phosphatase (Invitrogen™ 65-6122, 1:20,000 for H3 and 1:10,000 for H3K4me1). Detection was performed with an exposure time of 285 s, and the H3 band is observed within the expected molecular weight range of 15 to 17 kDa.

Bimolecular Fluorescence Complementation. For transfection and protein expression, saturated cultures of *Agrobacterium tumefaciens* GV3.101 encompassing plasmids of interest were washed twice and resuspended in an infiltration medium containing 20 mM MES (pH 5.2), 20 mM MgClâ and 150 μM acetosyringone. The bacterial cultures were adjusted to an OD_{600} of 0.3 and coincubated for 1 h at room temperature, with shaking, before being infiltrated into 3 to 4-wk-old *Nicotiana benthamiana* leaves. Fluorescence imaging was performed 3 d after agroinfiltration using an LSM880 ZEISS confocal microscope, equipped with a x20 objective. YFP was excited at 514 nm, and emission was detected between 515 and 580 nm. Chlorophyll autofluorescence was also detected between 670 and 735 nm. Images were acquired and analyzed using the Zen software.

RNA-Seq Experiments. For standard RNA-seq, total RNA was extracted from the meristematic zone and the first two leaves of thirty 7-d-old plantlets with the NucleoSpin RNA-Plus Kit (Macherey-Nagel) according to the manufacturer's instructions. For spike-in RNAseq, total RNA was extracted from 400 K nuclei using the TRIZol reagent (Invitrogen) according to the manufacturer's instructions. For both types of experiments, libraries were prepared with 2 μg of total RNA thanks to the NEBNext Ultra II RNA Library Prep Kit for Illumina according to the manufacturer's instructions. Differential Expression analysis was performed as described in (69) for standard RNA-seq and in (41) for spike-in RNAseq. Detailed procedure and analysis methods can be found in *SI Appendix*.

ChIP-seq experiments. ChIP-seq experiments and analyses were done as described in (69). Detailed procedure and analysis methods can be found in *SI Appendix*.

Affinity purification and Mass Spectrometry analysis (AP-MS). To do this experiment, we followed the protocol described in (42, 43). Detailed procedure and analysis methods can be found in *SI Appendix*. For this project, an *Arabidopsis* PSB-D cell culture expressing C-terminally GS^{rhino}-tagged LD under control of the estradiol-inducible XVE promoter was prepared. Detailed procedure and analysis methods can be found in *SI Appendix*.

Data, Materials, and Software Availability. ChIP-seq raw data are available at https://www.ncbi.nlm.nih.gov/geo/query/acc.cgi?acc=GSE292381 (70). RNAseq raw data are available at https://www.ncbi.nlm.nih.gov/geo/query/acc.cgi?acc=GSE292906 (71). AP-MS results are available at the

PRIDE repository (http://www.ebi.ac.uk/pride) with the accession number PXD065507 (72).

ACKNOWLEDGMENTS. This work was supported by grants of Agence Nationale de la Recherche (21-CE20-0027), a PhD fellowship from the University Paris-Saclay to Clara Bergis-Ser, Chinese Research Council Scholarships for Qingyi Wang and Xiaoning He, and a grant from the Fondation pour la Recherche Médicale (ECO201806006824) for Maherun Nisa. IPS2 benefits from the support of Saclay Plant Sciences-SPS (ANR-17-EUR-0007). BIFC plasmids were a kind gift of Dr François Parcy (LPCV, Grenoble, France). We thank Fredy Barnèche for stimulating discussions and critical reading of the manuscript. We thank the VIB Proteomics Core and Dominique Eeckhout for the LC-MSMS analyses.

Author affiliations: [a]Université Paris-Saclay, CNRS, Institut National de Recherche pour l'Agriculture, l'Alimentation et l'Environnement, Univ Evry, Institute of Plant Sciences Paris-Saclay, Orsay 91405, France; [b]Department of Plant Biotechnology and Bioinformatics, Ghent University, Ghent B-9052, Belgium; [c]Vlaams Instituut voor Biotechnologie, Center for Plant Systems Biology, Ghent B-9052, Belgium; [d]School of Life Science, University of Warwick, Coventry CV4 7AL, United Kingdom; [e]Sorbonne Université, CNRS, INSERM, Development, Adaptation and Ageing, Paris 75005, France; [f]Sorbonne Université, CNRS, Inserm, Institut de Biologie Paris-Seine, Paris 75005, France; [g]Université Paris Cité, Institute of Plant Sciences Paris-Saclay, Gif-sur-Yvette 91190, France; and [h]Institut Universitaire de France, Orsay 91400, France

1. C. Bergis-Ser *et al.*, Chromatin dynamics and RNA metabolism are double-edged swords for the maintenance of plant genome integrity. *Nat. Plants* **10**, 857–873 (2024).
2. K. R. Browning, H. Merrikh, Replication-transcription conflicts: A perpetual war on the chromosome. *Annu. Rev. Biochem.* **93**, 21–46 (2024).
3. H. Gaillard, T. García-Muse, A. Aguilera, Replication stress and cancer. *Nat. Rev. Cancer* **15**, 276–289 (2015).
4. L. M. Herr, E. D. Schaffer, K. F. Fuchs, A. Datta, R. M. Brosh, Replication stress as a driver of cellular senescence and aging. *Commun. Biol.* **7**, 616 (2024).
5. J. Herbst, Q.-Q. Li, L. De Veylder, Mechanistic insights into DNA damage recognition and checkpoint control in plants. *Nat. Plants* **10**, 539–550 (2024).
6. J. A. Pedroza-Garcia *et al.*, Function of the plant DNA polymerase epsilon in replicative stress sensing, a genetic analysis. *Plant Physiol.* **173**, 1735–1749 (2017).
7. M. Nisa *et al.*, Distinctive and complementary roles of E2F transcription factors during plant replication stress responses. *Mol. Plant* **16**, 1269–1282 (2023).
8. T. Pan *et al.*, A novel WEE1 pathway for replication stress responses. *Nat. Plants* **7**, 209–218 (2021).
9. L. Wang *et al.*, The ATR-WEE1 kinase module inhibits the MAC complex to regulate replication stress response. *Nucleic Acids Res.* **49**, 1411–1425 (2021).
10. W. Bao *et al.*, Protein kinase ATR inhibits E3 ubiquitin ligase CRL4PRL1 to stabilize ribonucleotide reductase in response to replication stress. *Cell Rep.* **42**, 112685 (2023).
11. K. M. Culligan, C. E. Robertson, J. Foreman, P. Doerner, A. B. Britt, ATR and ATM play both distinct and additive roles in response to ionizing radiation. *Plant J.* **48**, 947–961 (2006).
12. M. Szurman-Zubrzycka *et al.*, ATR, a DNA damage signaling kinase, is involved in aluminum response in barley. *Front. Plant Sci.* **10**, 1299 (2019).
13. J. A. Pedroza-Garcia *et al.*, Maize ATR safeguards genome stability during kernel development to prevent early endosperm endocycle onset and cell death. *Plant Cell* **33**, 2662–2684 (2021).
14. T. García-Muse, A. Aguilera, R. Loops, From physiological to pathological roles. *Cell* **179**, 604–618 (2019).
15. L. Goehring, T. T. Huang, D. J. Smith, Transcription-replication conflicts as a source of genome instability. *Annu. Rev. Genet.* **57**, 157–179 (2023).
16. H. Merrikh, Y. Zhang, A. D. Grossman, J. D. Wang, Replication-transcription conflicts in bacteria. *Nat. Rev. Microbiol.* **10**, 449–458 (2012).
17. C.-Y. Cho, J. P. Kemp, R. J. Duronio, P. H. O'Farrell, Coordinating transcription and replication to mitigate their conflicts in early *Drosophila* embryos. *Cell Rep.* **41**, 111507 (2022).
18. D. G. Wansink *et al.*, RNA polymerase II transcription is concentrated outside replication domains throughout S-phase. *J. Cell Sci.* **107**, 1449–1456 (1994).
19. M. Meryet-Figuiere *et al.*, Temporal separation of replication and transcription during S-phase progression. *Cell Cycle* **13**, 3241–3248 (2014).
20. M.-N. Prioleau, D. M. MacAlpine, DNA replication origins-where do we begin?. *Genes Dev.* **30**, 1683–1697 (2016).
21. S. Scaramuzza *et al.*, TRAIP resolves DNA replication-transcription conflicts during the S-phase of unperturbed cells. *Nat. Commun.* **14**, 5071 (2023).
22. A. Bayona-Feliu, A. Aguilera, Transcription-replication conflicts: Unlocking new frontiers in cancer. *Bioessays* **47**, e70025 (2025), 10.1002/bies.70025.
23. B. Jamge *et al.*, Histone variants shape chromatin states in *Arabidopsis*. *eLife* **12**, RP87714 (2023).
24. A.-S. Fiorucci *et al.*, *Arabidopsis* S2Ib links AtCOMPASS-like and SDG2 activity in H3K4me3 independently from histone H2B monoubiquitination. *Genome Biol.* **20**, 100 (2019).
25. S. Haider, S. Farrona, Decoding histone 3 lysine methylation: Insights into seed germination and flowering. *Curr. Opin. Plant Biol.* **81**, 102598 (2024).
26. I. Lee *et al.*, Isolation of *LUMINIDEPENDENS*: A gene involved in the control of flowering time in *Arabidopsis*. *Plant Cell* **6**, 75–83 (1994).
27. M. J. Aukerman, I. Lee, D. Weigel, R. M. Amasino, The *Arabidopsis* flowering-time gene LUMINIDEPENDENS is expressed primarily in regions of cell proliferation and encodes a nuclear protein that regulates LEAFY expression. *Plant J.* **18**, 195–203 (1999).
28. D. Jiang, W. Yang, Y. He, R. M. Amasino, *Arabidopsis* relatives of the human lysine-specific demethylase1 repress the expression of *FWA* and *FLOWERING LOCUS C* and thus promote the floral transition. *Plant Cell* **19**, 2975–2987 (2007).
29. R. Blanc-Mathieu, R. Dumas, L. Turchi, J. Lucas, F. Parcy, Plant-TFClass: A structural classification for plant transcription factors. *Trends Plant Sci.* **29**, 40–51 (2023), 10.1016/j.tplants.2023.06.023.
30. P.-L. Qi *et al.*, Characterization of an autonomous pathway complex that promotes flowering in *Arabidopsis*. *Nucleic Acids Res.* **50**, 7380–7395 (2022).
31. X. Fang *et al.*, The 3′ processing of antisense RNAs physically links to chromatin-based transcriptional control. *Proc. Natl. Acad. Sci. U.S.A.* **117**, 15316–15321 (2020).
32. C. Xu *et al.*, R-loop resolution promotes co-transcriptional chromatin silencing. *Nat. Commun.* **12**, 1790 (2021).
33. S. Inagaki, M. Takahashi, K. Takashima, S. Oya, T. Kakutani, Chromatin-based mechanisms to coordinate convergent overlapping transcription. *Nat. Plants* **7**, 295–302 (2021).
34. C. L. Baxter, S. Šviković, J. E. Sale, C. Dean, S. Costa, The intersection of DNA replication with antisense 3′ RNA processing in *Arabidopsis FLC* chromatin silencing. *Proc. Natl. Acad. Sci. U.S.A.* **118**, e2107483118 (2021).
35. I. Del Olmo *et al.*, Early in short days 7 (ESD7) encodes the catalytic subunit of DNA polymerase epsilon and is required for flowering repression through a mechanism involving epigenetic gene silencing. *Plant J.* **61**, 623–636 (2010).
36. A. Colon-Carmona, R. You, T. Haimovitch-Gal, P. Doerner, Technical advance: Spatio-temporal analysis of mitotic activity with a labile cyclin-GUS fusion protein. *Plant J* **20**, 503–508 (1999).
37. M. Sawa, S. A. Kay, GIGANTEA directly activates Flowering Locus T in *Arabidopsis thaliana*. *Proc. Natl. Acad. Sci. U.S.A.* **108**, 11698–11703 (2011).
38. K. Hayashi, J. Hasegawa, S. Matsunaga, The boundary of the meristematic and elongation zones in roots: Endoreduplication precedes rapid cell expansion. *Sci. Rep.* **3**, 2723 (2013).
39. J. Lovén *et al.*, Revisiting global gene expression analysis. *Cell* **151**, 476–482 (2012).
40. C. Evans, J. Hardin, D. M. Stoebel, Selecting between-sample RNA-seq normalization methods from the perspective of their assumptions. *Brief. Bioinform.* **19**, 776–792 (2018).
41. G. Schivre *et al.*, Genome-scale transcriptome augmentation during Arabidopsis thaliana photomorphogenesis. *Nat. Commun.*, in press.
42. J. Van Leene *et al.*, Mapping of the plant SnRK1 kinase signalling network reveals a key regulatory role for the class II T6P synthase-like proteins. *Nat. Plants* **8**, 1245–1261 (2022).
43. F. Persyn *et al.*, A nitrogen-specific interactome analysis sheds light on the role of the SnRK1 and TOR kinases in plant nitrogen signaling. *Mol. Cell. Proteomics* **23**, 100842 (2024).
44. E. Mateo-Bonmatí *et al.*, A CPF-like phosphatase module links transcription termination to chromatin silencing. *Mol. Cell* **84**, 2272–2286.e7 (2024).
45. S. N. Freytes, M. L. Gobbini, P. D. Cerdán, The plant mediator complex in the initiation of transcription by RNA polymerase II. *Annu. Rev. Plant Biol.* **75**, 211–237 (2024).
46. Z. Lai *et al.*, MED18 interaction with distinct transcription factors regulates multiple plant functions. *Nat. Commun.* **5**, 3064 (2014).
47. B. Bartkowiak, A. L. Greenleaf, Phosphorylation of RNAPII: To P-TEFb or not to P-TEFb? *Transcription* **2**, 115 (2011).
48. D. van den Heuvel, Y. van der Weegen, D. E. C. Boer, T. Ogi, M. S. Luijsterburg, Transcription-coupled DNA repair: From mechanism to human disorder. *Trends Cell Biol.* **31**, 359–371 (2021).
49. B. Xhemalçe, K. M. Miller, N. Gromak, Epitranscriptome in action: RNA modifications in the DNA damage response. *Mol. Cell* **84**, 3610–3626 (2024).
50. G. Cossa, P. K. Parua, M. Eilers, R. P. Fisher, Protein phosphatases in the RNAPII transcription cycle: Erasers, sculptors, gatekeepers, and potential drug targets. *Genes Dev.* **35**, 658–676 (2021).
51. J. Guo *et al.*, The CBP/p300 histone acetyltransferases function as plant-specific MEDIATOR subunits in *Arabidopsis*. *J. Integr. Plant Biol.* **63**, 755–771 (2021).
52. H. Takahashi *et al.*, Human mediator subunit MED26 functions as a docking site for transcription elongation factors. *Cell* **146**, 92–104 (2011).
53. O. Calvo, RNA polymerase II phosphorylation and gene looping: New roles for the Rpb4/7 heterodimer in regulating gene expression. *Curr. Genet.* **66**, 927–937 (2020).
54. M. A. Cortazar *et al.*, Control of RNA Pol II speed by PNUTS-PP1 and Spt5 dephosphorylation facilitates termination by a "sitting duck torpedo" mechanism. *Mol. Cell* **76**, 896–908.e4 (2019).
55. K. Cermakova *et al.*, A ubiquitous disordered protein interaction module orchestrates transcription elongation. *Science* **374**, 1113–1121 (2021).
56. J. R. Kelley *et al.*, The PNUTS phosphatase complex controls transcription pause release. *Mol. Cell* **84**, 4843–4861.e8 (2024).
57. Z. Wang *et al.*, The phosphatase PP1 sustains global transcription by promoting RNA polymerase II pause release. *Mol. Cell* **84**, 4824–4842.e7 (2024).
58. Y.-F. Han *et al.*, SUVR2 is involved in transcriptional gene silencing by associating with SNF2-related chromatin-remodeling proteins in *Arabidopsis*. *Cell Res.* **24**, 1445–1465 (2014).
59. F. Qian *et al.*, The GTE4–EML chromatin reader complex concurrently recognizes histone acetylation and H3K4 trimethylation in *Arabidopsis*. *Plant Cell* **37**, koae330 (2025).
60. W. Zong *et al.*, DEK domain-containing proteins control flowering time in *Arabidopsis*. *New Phytol.* **231**, 182–192 (2021).
61. D. Gökbuget *et al.*, Transcriptional repression upon S phase entry protects genome integrity in pluripotent cells. *Nat. Struct. Mol. Biol.* **30**, 1561–1570 (2023).
62. M. Lalonde, M. Trauner, M. Werner, S. Hamperl, Consequences and resolution of transcription-replication conflicts. *Life* **11**, 637 (2021).
63. R. Bhowmick, K. P. M. Mehta, M. Lerdrup, D. Cortez, Integrator facilitates RNAPII removal to prevent transcription-replication collisions and genome instability. *Mol. Cell* **83**, 2357–2366.e8 (2023).
64. H. B. Landsverk *et al.*, WDR82/PNUTS-PP1 prevents transcription-replication conflicts by promoting RNA polymerase II degradation on chromatin. *Cell Rep.* **33**, 108469 (2020).
65. A. Lampropoulos *et al.*, Greengate–A novel, versatile, and efficient cloning system for plant transgenesis. *PLoS One* **8**, e83043 (2013).
66. K. Yperman *et al.*, Molecular architecture of the endocytic TPLATE complex. *Sci. Adv.* **7**, eabe7999 (2021).
67. S. J. Clough, A. F. Bent, Floral dip: a simplified method for Agrobacterium-mediated transformation of Arabidopsis thaliana. *Plant J.* **16**, 735–743 (1998), 10.1046/j.1365-313x.1998.00343.x.
68. D. A. Ni *et al.*, The *Arabidopsis MCM2* gene is essential to embryo development and its over expression alters root meristem function. *New Phytol.* **184**, 311–322 (2009), 10.1111/j.1469-8137.2009.02961.x.

69. M. Nisa *et al.*, Distinctive and complementary roles of E2F transcription factors during plant replication stress responses. BioRxiv Revis. *Mol. Plant* **16**, 1269–1282 (2023), 10.1101/2023.01.06.523015.
70. C. Bergis-Ser *et al.*, The LUMINIDEPENDENS protein is a general repressor of transcription in Arabidopsis [LD ChIP-Seq]. NCBI GEO. https://www.ncbi.nlm.nih.gov/geo/query/acc.cgi?acc=GSE292381. Deposited 19 March 2025.
71. C. Bergis-Ser *et al.*, The LUMINIDEPENDENS protein is a general repressor of transcription in Arabidopsis [RNA-Seq 2]. NCBI GEO. https://www.ncbi.nlm.nih.gov/geo/query/acc.cgi?acc=GSE292906. Deposited 25 March 2025.
72. C. Bergis-Ser *et al.*, The LUMINIDEPENDENS protein is a general repressor of transcription in Arabidopsis. PRIDE repository. https://www.ebi.ac.uk/pride/archive/projects/PXD065507. Deposited 26 June 2025.